Type 1 and Type 3 Ryanodine Receptors Generate Different Ca^{2+} Release Event Activity in Both Intact and Permeabilized Myotubes

Christopher W. Ward,* Feliciano Protasi,† Daniel Castillo,† Yaming Wang,† S. R. Wayne Chen,‡ Isaac N. Pessah,§ Paul D. Allen,† and Martin F. Schneider*

*Department of Biochemistry and Molecular Biology, University of Maryland School of Medicine, Baltimore, Maryland 21201 USA, †Department of Anesthesia, Brigham and Women's Hospital, Boston, Massachusetts 02115 USA, ‡Department of Biochemistry and Molecular Biology, University of Calgary, Alberta T2N 1N4, Canada, and §Department of Molecular Biosciences, School of Veterinary Medicine, University of California, Davis, California 95616 USA

ABSTRACT In this investigation we use a "dyspedic" myogenic cell line, which does not express any ryanodine receptor (RyR) isoform, to examine the local Ca^{2+} release behavior of RyR3 and RyR1 in a homologous cellular system. Expression of RyR3 restored caffeine-sensitive, global Ca^{2+} release and causes the appearance of relatively frequent, spontaneous, spatially localized elevations of [Ca^{2+}], as well as occasional spontaneous, propagating Ca^{2+} release, in both intact and saponin-permeabilized myotubes. Intact myotubes expressing RyR3 did not, however, respond to K^+ depolarization. Expression of RyR1 restored depolarization-induced global Ca^{2+} release in intact myotubes and caffeine-induced global release in both intact and permeabilized myotubes. Both intact and permeabilized RyR1-expressing myotubes exhibited relatively infrequent spontaneous Ca^{2+} release events. In intact myotubes, the frequency of occurrence and properties of these RyR1-induced events were not altered by partial K^+ depolarization or by application of nifedipine, suggesting that these RyR1 events are independent of the voltage sensor. The events seen in RyR1-expressing myotubes were spatially more extensive than those seen in RyR3-expressing myotubes; however, when analysis was limited to spatially restricted "Ca^{2+} spark"-like events, events in RyR3-expressing myotubes were larger in amplitude and duration compared with those in RyR1. Thus, in this skeletal muscle context, differences exist in the spatiotemporal properties and frequency of occurrence of spontaneous release events generated by RyR1 and RyR3. These differences underscore functional differences between the Ca^{2+} release behavior of RyR1 and RyR3 in this homologous expression system.

INTRODUCTION

During depolarization of skeletal muscle, dihydropyridine receptor (DHPR)-voltage sensors of the transverse tubule (TT) membrane initiate Ca^{2+} release via the apposed ryanodine receptor (RyR) Ca^{2+} release channels in the sarcoplasmic reticulum (SR) membrane (Schneider and Chandler, 1973; Rios and Brum, 1987). In addition to such direct activation of Ca^{2+} release channels by TT voltage sensors, local Ca^{2+} elevations from voltage sensor-induced release may activate other nearby RyR Ca^{2+} release channels (Block et al., 1988; Rios and Pizarro, 1988; Csernoch et al., 1993) through a Ca^{2+}-induced Ca^{2+} release pathway (CICR) (Meissner, 1994).

Two different RyR isoforms, RyR1 and RyR3, have been found to be expressed in skeletal muscle. Whereas RyR1 is the predominant isoform in adult mammalian skeletal muscle, RyR3 is widely distributed through most skeletal muscles during development and is found in limited amounts in respiratory muscle and slow twitch limb muscle in mature animals (Conti et al., 1996; Bertocchini et al., 1997; Flucher et al., 1999). From experiments with RyR1-null mice, it is known that RyR1 is required for normal voltage-dependent skeletal type excitation-contraction (E-C) coupling (Nakai et al., 1996). Additionally, experiments with dyspedic 1B5 myotubes virally transduced with RyRs have demonstrated that RyR1, but not RyR3, restores both the tetradic arrangement of DHPRs (Protasi et al., 1998, 2000) and depolarization-induced Ca^{2+} release (Fessenden et al., 2000). RyR3, in contrast, has been proposed to augment the voltage-initiated RyR1 Ca^{2+} release in skeletal muscles through CICR mechanisms (Sonnleitner et al., 1998).

RyR channel activity in muscle gives rise to discrete, localized elevations of myoplasmic [Ca^{2+}], Ca^{2+} "sparks," (Cheng et al., 1993) which are thought to represent fundamental units of SR Ca^{2+} release (Cannell et al., 1999; Shirokova, et al., 1999a; Schneider, 1999). These discrete events arise from a small number of RyR channels constituting a functional Ca^{2+} release unit (Shirokova et al., 1999a; Shtifman et al., 2000; Brum et al., 2000). Several reports have demonstrated that Ca^{2+} sparks are readily detected in frog skeletal muscle (Tsugorka et al., 1995; Klein et al., 1996) and in embryonic mammalian skeletal muscle (Chun et al., 2001; Shirokova et al., 1998, 1999b; Conklin et al., 2000). However, sparks are either not detected (Shirokova et al., 1998) or occur very infrequently in adult mammalian skeletal muscle (Conklin et al., 1999b; Chun et al., 2001). Based on the fact that embryonic mammalian skeletal muscle and frog skeletal muscle express two RyR isoforms (RyR1 and RyR3 or amphibian/avian homologs $\propto$ and β, respectively) (Sutko and Airey, 1996),

Received for publication 5 December 2000 and in final form 17 September 2001.

Address reprint requests to Dr. Martin F. Schneider, Department of Biochemistry and Molecular Biology, University of Maryland School of Medicine, Baltimore MD 21201. Tel.: 410-706-5787; Fax: 410-706-8297; E-mail: mschneid@umaryland.edu.

0006-3495/01/12/3216/15 $2.00

whereas most adult mammalian muscles express only the RyR1 isoform (Conti et al., 1996), the likelihood of occurrence of discrete, spatially isolated, Ca^{2+} release events could be isoform-dependent.

Myotubes cultured from the dyspedic 1B5 myogenic cell line lack all expression of any RyR, but still express key skeletal muscle E-C coupling components (Moore et al., 1998). These myotubes exhibit no forms of Ca^{2+} release in response to caffeine, 4-chloro-*m*-cresol, or K^+ or electrical depolarization. Expression of either RyR3 or RyR1 cDNA in these dyspedic myotubes restored Ca^{2+} release in response to caffeine application, which is the hallmark of CICR (Moore et al., 1998; Fessenden et al., 2000; Nakai et al., 1996). Recently, our laboratories have used this expression system to show that expression of RyR3 in these dyspedic myotubes is sufficient to produce discrete, localized Ca^{2+} release events (Ward et al., 2000). These events, imaged in permeabilized myotubes loaded with 50 μm fluo-3, were similar to Ca^{2+} spark-type release events seen in frog skeletal muscle (Ward et al., 2000).

In the present study we have used dyspedic 1B5 myotubes to investigate the elemental Ca^{2+} release behavior of RyR3, RyR1, and $RyR3_m$, a Ca^{2+}-insensitive RyR3 mutant (Chen et al., 1999), in an attempt to further elucidate the elementary Ca^{2+} release behavior of the skeletal muscle RyR isoforms. We now show that expression of RyR3 causes the appearance of frequent spontaneous Ca^{2+} release events in both intact and permeabilized myotubes, with the events being spatially somewhat more extensive in the intact myotubes. In addition, we report that expression of RyR1 causes infrequent spontaneous events, which are more spatially extensive than those seen with RyR3 in either intact or permeabilized myotubes. Expression of $RyR3_m$ does not restore any form of Ca^{2+} release. Thus, in the context of skeletal muscle, RyR3 and RyR1 alone are each sufficient to produce highly localized spontaneous Ca^{2+} release events. The observed differences in the frequency of occurrence and the spatiotemporal characteristics of the events seen between RyR3 and RyR1 suggest differences in Ca^{2+} release behavior of the two RyR isoforms in skeletal muscle.

METHODS

Cell Culture

1B5 cells (RyR null) (Moore et al., 1998) were cultured in opticlear 96-well plates (Costar, Silicon Valley, CA) in DMEM medium with 20% fetal bovine serum, 100 μg/ml streptomycin sulfate, 100 units/ml penicillin-G, 5% CO_2. This cell line has previously been shown to lack expression of all RyR isoforms (Moore et al., 1998). Cells were then allowed to differentiate into myotubes (5–7 days) in a low growth factor medium (no fetal bovine serum) containing 5% heat-inactivated horse serum, 23% CO_2, pH ~7.05.

Differentiated myotubes were exposed to helper-free herpes simplex virus (HSV)-1 amplicon virions (Wang et al., 2000; Fraefel et al., 1996) containing cDNA for RyR3, RyR1, or RyR3 mutant ($RyR3_m$; E3885A) (Chen et al., 1999) for 1–2 h at a moiety of infection of ~1. Myotubes were then cultured for 24–36 h in differentiation medium before imaging for functional Ca^{2+} release.

Confocal fluorescence imaging of Ca^{2+} indicators

Differentiated myotubes from RyR-infected cultures were examined either intact or after chemical permeabilization. Intact myotubes were loaded for 15–30 min with 10 μm fluo-4 acetoxymethyl ester (AM) in Krebs Ringer solution. After the loading protocol, the cells were allowed to rest (~20–30min) in Krebs Ringer without the fluorescent dye. Myotubes that underwent chemical permeabilization were exposed to saponin (12 μg/ml; 30 s) in internal solution (mM; 95 Cs-glutamate, 20 creatine phosphate, 4.5 Na-tris-maleate, 13.2 Cs-tris-maleate, 5 glucose, 0.1 EGTA, 1 DTT, 0.18–0.42 Mg^{2+}; ~100 nM free Ca^{2+}), washed in internal solution, then bathed in internal solution containing 50 μM fluo-3 (pentapotassium salt). In both conditions, cells were monitored for functional Ca^{2+} release at 37°C in a custom-built air-jacketed chamber (Ward et al., 2000) on an inverted microscope (Olympus IX-70 60×-1.4 na oil or 60×-1.3 na water objective; Olympus, Hamburg, Germany). This was coupled to a laser scanning confocal system (488 nm excitation; Bio-Rad MRC-600, Bio-Rad, Hercules, CA) used in either *xy* or in linescan *xt* mode (1 s acquisition time; 2 ms/line, 768 pixels per line). The confocal aperture was set to 25% of maximal setting; the resolution was estimated at 0.4 μm in the *x* and *y* dimensions and 0.8 μm in the *z* dimension. In all confocal images presented here, the *x* scan distance is represented as vertical displacement and the horizontal displacement represents either the *y* scan distance in the *xy* images or time in the *xt* linescan images.

Linescan (*xt*) and full frame (*xy*) images were processed and fluorescence fluctuations identified using custom software programs based on the autodetection algorithm modified from Cheng et al. (1999). In brief, myotube cultures were screened for locations of spark generation by monitoring 30–50 successive *xy* confocal fluorescence images of a randomly selected field containing several myotubes. In a manually defined region-of-interest encompassing a single myotube, a series of successive images of each field were summed and averaged to generate an average fluorescence image (F) which was then subtracted from each image in the series to create a change in fluorescence image (ΔF). Potential regions of Ca^{2+} release were computer identified as contiguous areas of interest with fluorescence $\geq$ 2 SD above the mean F and corresponding pixel locations were stored. The F image was then recalculated to ignore regions of locally elevated fluorescence in any image and ΔF images were recalculated. Potential Ca^{2+} release events areas were then reanalyzed and accepted as events if a portion of the 2-SD area reached a threshold $\geq$3 SD above the mean F. After conversion identification, ΔF images were divided, pixel by pixel, by the F image to give a $\Delta F/F$ image and regions of locally elevated fluorescence were then analyzed for peak amplitude and total area $\geq$50% of peak amplitude. Detected events were defined as having a peak amplitude of $\Delta F/F \geq 0.3$ and area (pixel area $\geq$50% of peak amplitude) ≥ 0.35 μm^2.

Linescan event selection and analysis was conducted using a modified computer method (Cheng et al., 1999) and detailed previously (Ward et al., 2000). Linescan (*xt*) images were converted to images of change in fluorescence (ΔF) by subtracting the average fluorescence (F) of the five sequential images at each spatial location from each raw fluorescence image. Each ΔF image was then divided by F to create a $\Delta F/F$ image. Ca^{2+} sparks in linescan were selected and analyzed. Events were accepted or rejected according to these criteria: a change in $\Delta F/F \geq 0.3$, full duration at half-maximal amplitude (FDHM) $\geq$6 ms, and full width at half-maximal amplitude (FWHM) ≥ 1 μm. The rise time of the events was taken as the time from 10–90% of the maximal amplitude. Results are expressed as mean ± SEM.

Immunohistochemistry

Both intact and permeabilized myotube preparations were methanol-fixed and stained with a monoclonal primary antibody (34C; Developmental Studies Hybridoma Bank, University of Iowa, IA, Airey et al., 1990) as previously described in detail (Ward et al., 2000). This antibody recognizes mammalian RyR1 and RyR3, as well as frog RyR$\propto/\beta$. Primary antibody labeling was followed by labeling with a CY3 conjugated goat anti-mouse secondary antibody (Jackson ImmunoResearch Laboratories, West Grove, PA). Nonconfocal fluorescent images were obtained using an Olympus IX70 epifluorescence microscope and either a 10 × 0.3 na or 100× oil 1.3 na plan apochromat objective.

Western blots

Control and HSVRyR1, or HSVRyR-infected 1B5 myotubes and adult chick or rabbit skeletal muscle were homogenized, loaded on top of a two-step 27%/45% sucrose gradient, and centrifuged at 40,000 × g (17,000 rpm) in a Beckman SW41 rotor (Beckman Instruments, Inc., Fullerton, CA) for 1 h. The fraction at the 27%/45% interface was collected, washed, pelleted, and resuspended in 10% sucrose buffer (10 mM HEPES, pH 7.4), frozen in liquid nitrogen, and stored at −80°C (8, 30). Western blot analysis was carried out on these samples that were size-separated on sodium dodecyl sulfate gels, transferred to PD polyvinylidene difluoride VF membranes, incubated with ab34C (Developmental Studies Hybridoma Bank, University of Iowa). The immunoreactive bands detected with enhanced chemiluminescent techniques (NEN Life Science Products, Boston, MA) as described previously (Moore et al., 1998).

[3H]ryanodine binding

Fifty μg SR protein (see Western blot methods) was incubated in a 500-μl binding buffer (250 mM KCL, 15 mM NaCl, 50 μM $CaCl_2$, 20 mM HEPES, pH 7.1, 10 nM [3H]ryanodine (60 Ci/mmol)) for 3 h at 37°C. Reaction media was filtered through GF/B glass fiber filters using Brandel Cell harvester (Gaithersburg, MD) and washed 2 × 5 ml with ice-cold buffer (20 mM Tris, 50 μM CaCl, pH 7.1).

Data analysis

Quantitative analysis of fluorescence images was performed with custom image analysis routines written in the IDL 5.0 (Boulder, CO). Statistical comparisons between response variables was conducted by an appropriate paired or nonpaired *t* test with significance set at the $P < 0.05$ level.

RESULTS

Patterns and levels of expression of RyR protein in RyR1- and RyR3-transduced myotubes

Myotube cultures were transduced with RyR1, RyR3, or the Ca^{2+}-insensitive E3885A RyR3 mutant, $RyR3_m$ (Chen et al., 1999) helper virus-free amplicon virions, and were examined for the level and pattern of RyR expression. Cultures were immunostained with ab34C, which labels both RyR1 and RyR3, and then with a Cy3 conjugated secondary antibody (Fig. 1). Transduced 1B5 myotubes expressed all three RyR proteins with similar frequency (Fig. 1, *A–C*, *top*) and the peripheral immunostaining pattern of all three (Fig. 1, *A–C*, *bottom*) is identical to what was shown previously for RyR1 (Protasi et al., 1998) and RyR3 (Ward et al., 2000; Protasi et al., 2000). The punctate expression pattern at the cell surface is attributable to a predominance of peripheral couplings between the SR and surface membrane because of the absence of a well formed *t*-tubular system in developing myotubes (Protasi et al., 1998)

Expression of functional RyR protein and the presence of a releasable pool of sequestered Ca^{2+} were assessed with a caffeine challenge (Fig. 1, *E–G*). Application of 15 mM caffeine resulted in a robust global elevation of cytosolic $[Ca^{2+}]$ in both the RyR1- and RyR3-transduced myotubes, confirming the proper targeting of functional RyR protein and the presence of a significant pool of stored Ca^{2+} releasable by CICR in myotubes expressing either RyR1 or RyR3. The expression efficiency of both RyR constructs was evaluated as the percentage of myotubes within a image field exhibiting global Ca^{2+} release after a 15-mM caffeine challenge under a wide field view (20× obj.). There was no difference in functional RyR expression between the myotubes transduced with RyR3 (67.8 ± 3.1%; $n = 5$ image fields) or RyR1 (62.2 ± 7.2%; $n = 4$ image fields). The mean value of the maximum relative change in cytosolic fluorescence ($\Delta F/F$) caused by exposure to caffeine was not different in intact RyR1- or RyR3-expressing myotubes (3.53 ± 0.45 or 3.19 ± 0.25, respectively). It was also not different in permeabilized RyR1- or RyR3-expressing myotubes (3.08 ± 0.52, 3.09 ± 0.46) ($P < 0.05$), indicating similar levels of SR Ca^{2+} loading in all myotubes. There was also no difference in values for either isoform before and after permeabilization. In contrast, myotubes transduced with the Ca^{2+}-insensitive RyR3 mutant never exhibited any detectable elevation of $[Ca^{2+}]$ in response to caffeine.

Membrane potential dependent activation of Ca^{2+} release was observed during depolarization by application of 40 mM K^+ Ringer's solution to intact RyR1-transduced myotubes (Fig. 1, *H–J*; fluo-4 AM), but not to RyR3- or $RyR3_m$-transduced myotubes, indicating that only RyR1 was capable of supporting skeletal type depolarization-induced E-C coupling (Fessenden et al., 2000). The depolarization-induced $[Ca^{2+}]_i$ elevation in RyR1-transduced myotubes provides further support for the presence of a substantial store of releasable Ca^{2+} in the RyR1-transduced myotubes.

Fig. 1 *K* presents a Western blot of the immunoreactive RyR1 and RyR3 protomer from the heavy SR fraction of virally transduced 1B5 myotube preparations. The RyR protein exhibited similar mobilities as RyR isolated from rabbit (RyR1) and avian (RyR1, RyR3) junctional SR. [^{3}H]ryanodine binding assays performed on RyR1 and RyR3 protein expressed in transduced, differentiated 1B5 cells were not different (493 ± 38 vs. 522 ± 18 fmol/mg SR protein, respectively; $n = 3$, ± SD), suggesting that

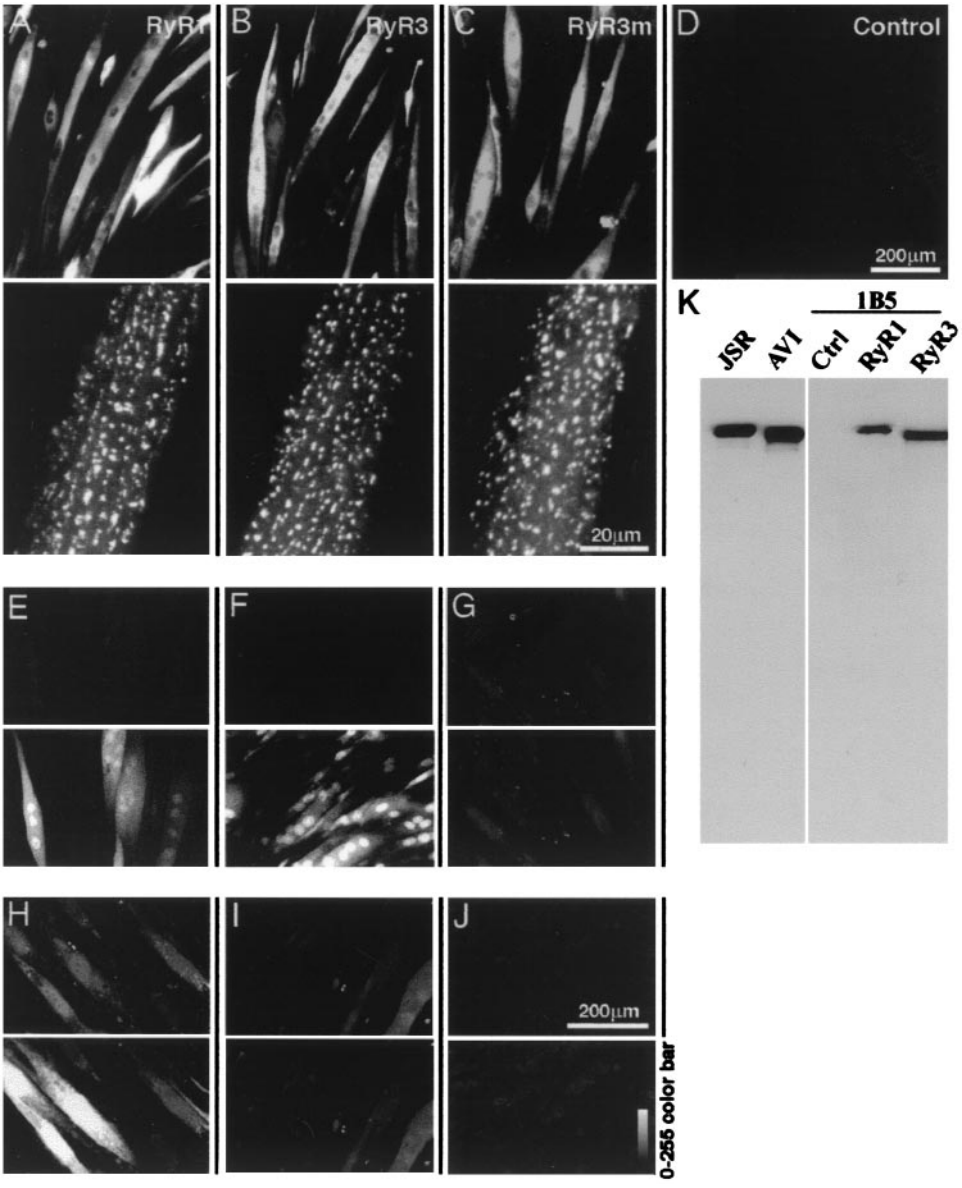

FIGURE 1 Expression of RyR protein and caffeine/potassium (K^+) responsiveness in 1B5 myotubes virally transduced with RyR cDNAs. Columns 1–3 contain differentiated 1B5 cells infected with RyR1, RyR3, and $RyR3_m$ virions. Cultures have been immunostained for RyR. (*A–C* (*top*)) display saponin-permeabilized 1B5 myotubes at 10× magnification. The lower panels of (*A–C*) display a corresponding 100× immunofluorescent image. (*D*) is a 10× immunofluorescent image of untransfected differentiated 1B5 cells. Immunofluorescence images of intact cells (i.e., without saponin treatment) were identical to the cells shown. (*E–G*) present *xy* confocal images before (*top*) and during (*bottom*) exposure to a 15-mM caffeine challenge. (*H–J*) are *xy* confocal images of intact myotubes before (*top*) and during (*bottom*) exposure to a 40 mM K^+ challenge. (*K*) is a Western blot of an entire sodium dodecyl sulfate-polyacrylamide gel electrophoresis gel of proteins isolated from rabbit and chicken JSR, and from heavy SR differentiated 1B5 cells (control, RyR1-infected, and RyR3-infected).

the amount of RyR protein expressed in both RyR3 and RyR1 transduced cells was not different.

Spontaneous local [Ca^{2+}] elevations in RyR3- and RyR1-transduced myotubes

Myotubes expressing either RyR3 or RyR1 exhibited spontaneous localized elevations in fluorescence. Fig. 2 displays pseudocolor surface plots of five representative successive $\Delta F/F$ normalized fluorescence *xy* images of RyR3- and RyR1-transduced myotubes that were permeabilized and bathed in standard internal solution containing the Ca^{2+} indicator fluo-3 (50 μm). Fluorescence fluctuations indicative of local elevations of [Ca^{2+}] are apparent in these $\Delta F/F$ images, which report change in fluorescence relative to the average fluorescence image of the entire series of images of

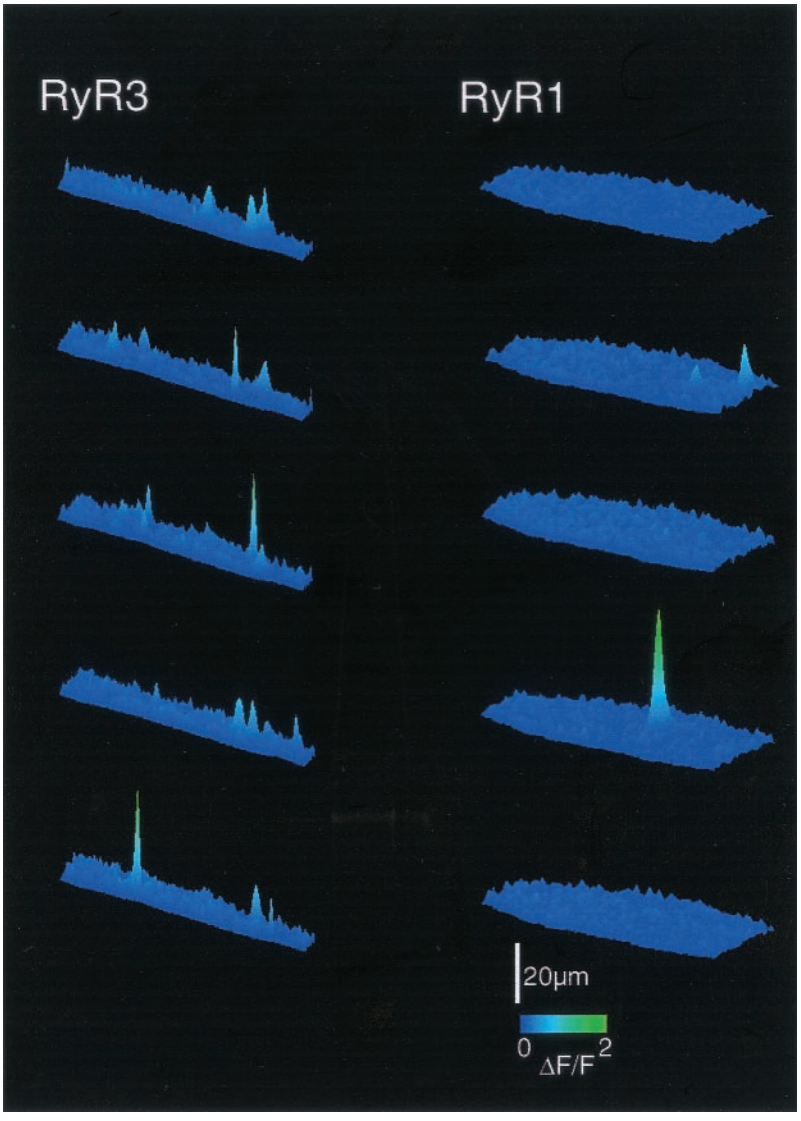

FIGURE 2 Successive *xy* scans from permeabilized and fluo-3–loaded RyR3- or RyR1-expressing myotubes are shown in a pseudocolor surface-plot presentation. For presentation purposes, five successive scans were selected from a series of 30–50 images. The area of each image series represents the visually identified boundaries of myotube within a 60× field. Transient fluorescence fluctuations, representing local Ca^{2+} release events, are indicated by the pseudocolored peaks.

the same field. These discrete fluctuations in fluorescence are empirically identified (see Methods) as isolated regions of increased fluorescence that appear transiently during successive images.

Frequency of occurrence of Ca^{2+} release events in RyR3- and RyR1-expressing myotubes

To objectively determine event frequency in the RyR-expressing myotubes, 30–50 successive confocal *xy* scans were collected in a given random field of myotubes in either intact or permeabilized myotube cultures and the event frequency was determined (Fig. 3). In intact RyR3-transduced myotubes loaded with fluo-4 AM, successive *xy* images of random fields within each culture dish (24 cultures; 84 random fields) revealed spontaneous local regions of increased fluorescence in at least one myotube in virtually every field examined. The overall frequency of occurrence of events in these RyR3-transduced myotubes was 0.92 ± 0.13 events per *xy* image. The frequency of occurrence of events was similar in RyR3 cultures that were saponin-permeabilized (separate cultures from intact preparations; 26 cultures; 94 random fields) and bathed in a standard internal solution (see Methods). These myotubes exhibited a Ca^{2+} release event frequency of 1.09 ± 0.26 events/image.

In contrast to the RyR3-expressing myotubes, the spontaneous Ca^{2+} release events in RyR1-expressing myotubes

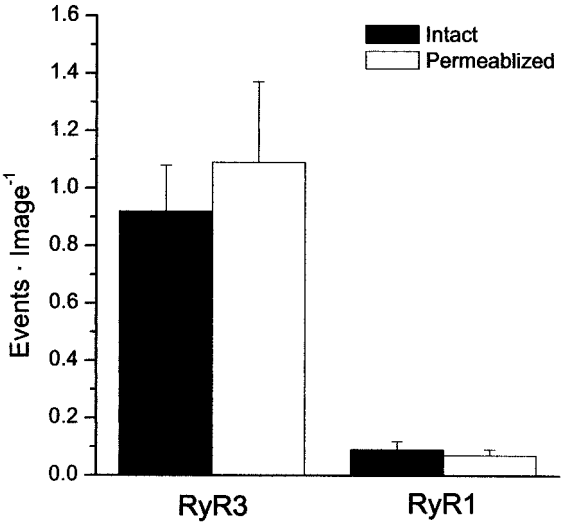

FIGURE 3 Frequency of occurrence of Ca^{2+} release events in RyR3- and RyR1-expressing 1B5 myotube cultures. Frequency was determined as the mean number of events identified in successive *xy* scans in random fields of myotube cultures (see Methods). Intact 1B5 myotube cultures transduced with RyR3 exhibited a lower frequency of spontaneous events (0.92 ± 0.13; 24 cultures, 84 random fields) than permeabilized myotubes (1.09 ± 0.26 events/image; 26 cultures, 94 random fields). Intact RyR1-expressing myotubes (0.09 ± 0.03 events/image; 44 fields in 16 cultures) exhibited a greater event frequency compared with permeabilized RyR1 expressing cultures (0.07 ± 0.02 events/image; 36 fields in 13 cultures).

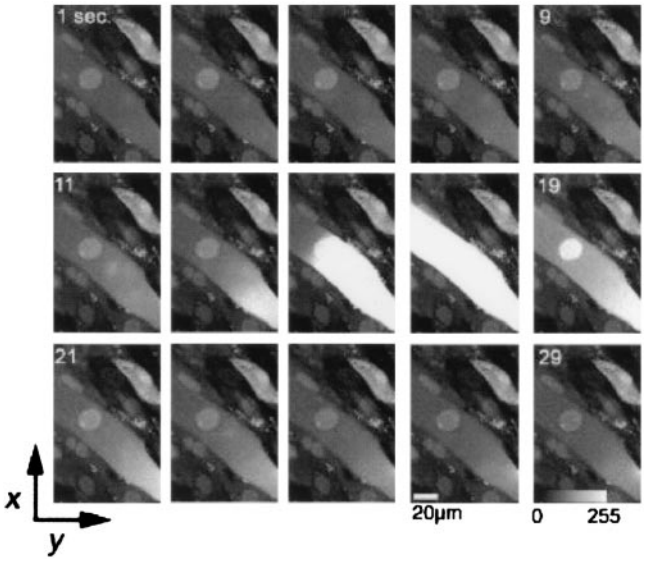

FIGURE 4 Spontaneous whole-cell Ca^{2+} wave in a permeabilized 1B5 myotube transduced with RyR1.

occurred at a very low rate. Spontaneous Ca^{2+} release events in intact RyR1-expressing cells (44 random fields in 16 cultures) were 0.09 ± 0.03 and 0.07 ± 0.02 events/image in the permeabilized (38 fields in 13 cultures) cultures, respectively. This represents a 10-fold lower frequency of event occurrence compared with RyR3. Partial depolarization of intact RyR1-transduced cultures, by increasing $[K^+]$ from the control level of 4 mM to 7 mM (0.16 ± 0.09 events/image; 9 random image fields in three cultures) had no effect on event frequency. Neither did application of 1 μM nifedipine (0.10 ± 0.22 events/image; 8 random image fields in three cultures). Thus, membrane voltage sensors and Ca^{2+} passing through the slow voltage gated Ca^{2+} channels do not seem to regulate the events that occurred in these intact RyR1-transduced myotubes. Similarly, the application of 0.5 and 1 mM caffeine (subcontracture threshold levels), which might be expected to increase the occurrence of ligand-activated Ca^{2+} release events, did not significantly alter the frequency of spontaneous Ca^{2+} release events in RyR1-expressing myotubes (0.16 ± 0.11; 10 random image fields in three cultures with 0.5 mM caffeine, 0.19 ± 0.21; 9 random image fields in three cultures with 1 mM caffeine), compared with control levels. This observation is consistent with previous reports of the relative insensitivity of RyR1 to the effects of caffeine compared with RyR3 during both local (Conklin et al., 1999a, b) and global (Fessenden et al., 2000; Bertocchinni et al., 1997) Ca^{2+} release. Application of 40 mM K^+ or 15 mM caffeine did elicit a global Ca^{2+} release in intact RyR1-transduced myotubes (Fig. 1), indicating that RyR1 expression in these cells did respectively restore both voltage-dependent skeletal DHPR-RyR E-C coupling mechanisms and CICR, as previously described in this 1B5 system (Protasi et al., 1998).

In permeabilized RyR1-transduced cultures, a reduction in internal solution free $[Mg^{2+}]$ (0.42 to 0.18mM; three myotubes) resulted in a global, reversible increase in myoplasmic fluorescence in three myotubes in which a discrete, spontaneous event was previously detected during visual inspection. This global fluorescence response indicates an increase in the relative rate of Ca^{2+} release compared with Ca^{2+} uptake in response to the lowered Mg^{2+}, consistent with activation of CICR on lowering $[Mg^{2+}]$. Despite visually identifying a discrete event before image acquisition, 20 successive images acquired in each condition revealed no discrete, spontaneous events. Thus, because of the low frequency of occurrence of these spontaneous events seen in RyR1-expressing myotubes, no conclusion can be drawn regarding the effect of $[Mg^{2+}]$ on RyR1 event frequency, although lowering myoplasmic $[Mg^{2+}]$ apparently increased CICR in RyR1-expressing myotubes. It is important to note, however, that despite the low occurrence of discrete events in RyR1 expressing myotubes, successive *xy* scans of intact (not shown) or permeabilized RyR1-infected myotubes did capture whole-cell Ca^{2+} release behavior as a wave of increased fluorescence spreading over the entire myotube without any discernible, discrete Ca^{2+} release events preceding the activity (Fig. 4).

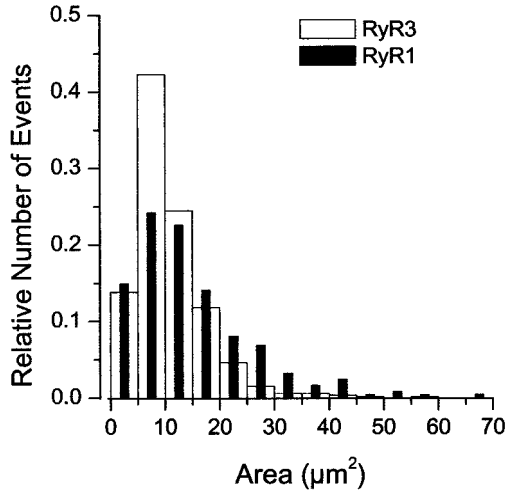

FIGURE 5 Spatial area histograms of Ca^{2+} release events identified in permeabilized RyR3- and RyR1-expressing myotubes. Event area was determined as the area of the event fluorescence (see Methods) >50% of the maximal $\Delta F/F$ of the event fluorescence. The mean area of events in the RyR3 expressing cultures ($10.8 \pm 0.2\ \mu m^2$, $n = 940$) was significantly smaller than the mean area of events in RyR1-expressing cultures ($15.01 \pm 0.7\ \mu m^2$, $n = 248$; $P < 0.05$).

Spatiotemporal properties of Ca^{2+} release events in RyR3- and RyR1-expressing myotubes

The spatial properties of the spontaneous Ca^{2+} release events generated by RyR1 and RyR3 were evaluated in the permeabilized myotube preparations. The permeabilized preparation provides the opportunity to apply a defined intracellular milieu for a detailed comparison of the properties of both isoforms and also negates any possible effect of the DHPR voltage sensor (Chandler et al., 1976) in initiating Ca^{2+} release events in the RyR1-expressing myotubes.

Initially, spatiotemporal properties were evaluated in the *xy* scans of the random fields used to determine event frequency. Fig. 5 displays a histogram of the Ca^{2+} release event area, which is defined as the area of identified fluorescence above 50% of the $\Delta F/F$ peak amplitude. The mean area of the population of Ca^{2+} release events was greater in the RyR1-expressing myotubes ($15.1 \pm 0.7\ \mu m^2$; $n = 248$) than the RyR3-expressing myotubes ($10.8 \pm 0.2\ \mu m^2$; $n = 940$, $P = 0.003$). However, the peak amplitude of the Ca^{2+} release events evaluated in *xy* images was similar between the RyR1 and RyR3 isoforms, respectively (1.18 ± 0.74 vs. $1.19 \pm 0.46\ \Delta F/F$).

To obtain a more precise spatiotemporal evaluation of the Ca^{2+} release events in RyR1- and RyR3-expressing myotubes, linescan imaging (2 ms/line) was used. As opposed to the random scanning of fields of myotubes used in the *xy* experiments, the low occurrence of events in the RyR3, and especially in the RyR1 myotubes, necessitated our visually identifying myotubes which had Ca^{2+} release activity before initiating linescan data collection.

Fig. 6 presents representative linescan image strips from permeabilized RyR3- and RyR1-expressing myotubes. Visual inspection revealed discrete, localized Ca^{2+} release events that occurred both as single events as well as in a repetitive fashion. The majority of the events had relatively rapid rising and decay kinetics reminiscent of the stereotypic Ca^{2+} spark-type release seen in numerous skeletal, cardiac, and smooth muscle preparations (Fig. 6 *A*). In addition, events were visualized which were non-spark-like. One subpopulation of these events had markedly slower timecourses (Fig. 6 *B*) of several hundred milliseconds and often were poorly defined in their rising and decay kinetics. An additional subpopulation comprised small Ca^{2+} waves that propagated from an initiating release site (Fig. 6 *C*). The total number of nonstereotypic events identified in linescan images represented 9% of the RyR3 ($n = 21$) events collected and 34% of the RyR1 events ($n = 52$) collected.

Fig. 7 presents histograms of the spatiotemporal properties of 246 and 151 Ca^{2+} release events collected in linescan images of RyR3 and RyR1 myotubes, respectively. It is important to note however, that the analysis of the spatiotemporal properties of localized Ca^{2+} release events in these histograms is limited to events that were spatially symmetric and well defined in their temporal kinetics (spark-like) which enabled analysis with our predefined criteria (see Methods). This population of events in RyR3 myotubes was ~20% larger in amplitude (1.15 ± 0.04 vs. 0.97 ± 0.03; $\Delta F/F$, $P < 0.05$) and longer in duration (17.48 ± 0.58 vs. 14.39 ± 0.36 ms FDHM, $P < 0.05$), but similar in rise time (7.68 ± 0.29 vs. 7.73 ± 0.29 ms) and spatial width (1.88 ± 0.05 vs. $1.80 \pm 0.04\ \mu m$ FWHM) when compared with the events imaged in RyR1-expressing myotubes.

Properties of Ca^{2+} release events in intact versus permeabilized RyR3-expressing myotubes

We compared the spatial and temporal properties of events in intact and permeabilized preparations to investigate the effect of permeabilization and introduction of the artificial intracellular milieu on the Ca^{2+} event properties. For this comparison, we chose RyR3-expressing myotubes because the frequency of occurrence of spontaneous events was robust in intact and permeabilized myotubes that exhibited event activity. Cultures of intact fluo-4 AM–loaded myotubes ($n = 8$) were examined for spontaneous activity, and individual myotubes were identified which had robust spontaneous activity. After evaluation of the Ca^{2+} release events, these myotubes were subsequently saponin-permeabilized. The myotubes were then exposed to 50 μm fluo-3 containing internal solution and re-imaged for spontaneous fluctuations in fluorescence. Fig. 8 displays four successive

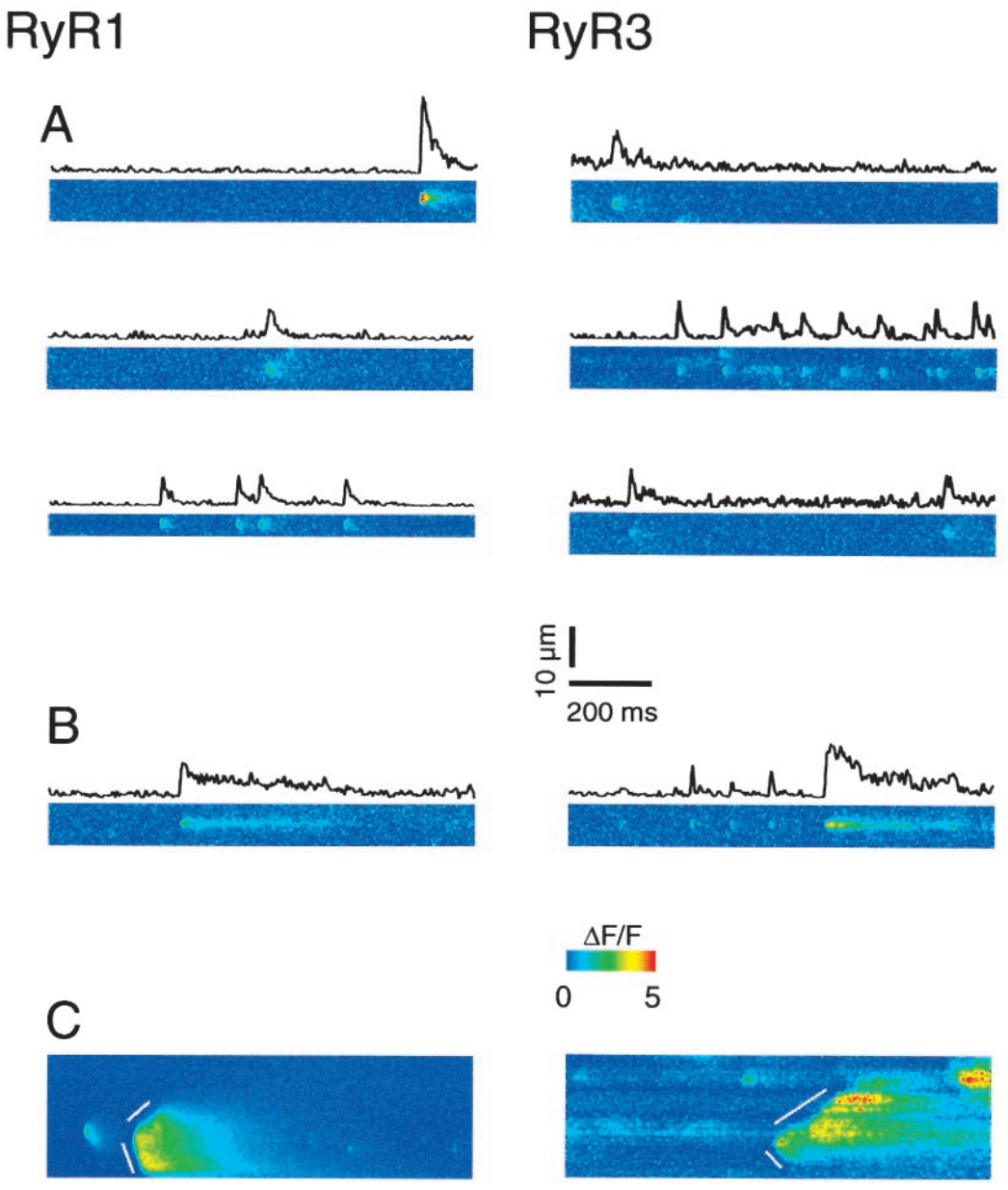

FIGURE 6 Image strips and temporal time courses of spontaneous Ca^{2+} release events imaged in RyR1- and RyR3-expressing 1B5 myotube cultures. Temporal time courses represent the average of three spatial pixels centered on the fluorescence peak in the image. (*A*) Discrete, spatially symmetric Ca^{2+} spark type release events were imaged in both permeabilized RyR3- and RyR1-expressing myotube cultures. (*B* and *C*) A number of events were collected in both RyR3 and RyR1 cultures which were nonsterotypic and could not be evaluated with our predefined criteria. These included spatially restricted, long-duration release events with poorly defined temporal kinetics (*B*) as well as spatially propagating Ca^{2+} waves that involved successive recruitment of calcium release units (*C*). The propagating fronts of the Ca^{2+} waves are highlighted with white bars.

$\Delta F/F$ *xy* images of the same intact (Fig. 8 *A*) and subsequently permeabilized (Fig. 8 *B*) myotube. The spontaneous fluorescence changes recorded in the permeabilized RyR3-infected myotubes seemed spatially less extensive and more sharply defined than the events in the same cell before permeabilization. Histograms of the areas of the events in *xy* images of the same intact (Fig. 8 *C*) and permeabilized (Fig. 8 *D*) RyR3-transduced myotubes demonstrate the difference in spatial extent of the events before and after permeabilization. The event areas are calculated as the total event area having $\Delta F/F$ pixel values greater than or equal to half the maximum $\Delta F/F$ in the same event. The intact RyR3-transduced myotubes exhibited a significant population of larger events (area >10 um^2, Fig. 8 *C*) that were not present after permeabilizing the same myotubes (Fig. 8 *D*). The mean values of event areas were 16.64 ± 2.64 and 4.02 ± 0.45 μm^2, before and after permeabilization ($P < 0.05$), respectively. Thus, the events observed after permeabilization

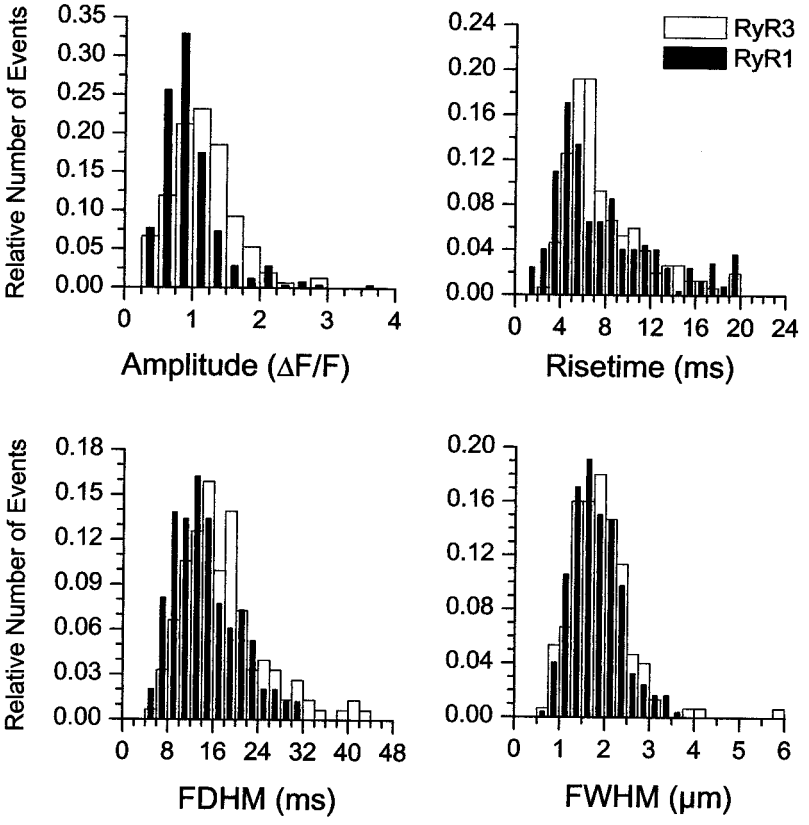

FIGURE 7 Histograms of the spatiotemporal properties of Ca^{2+} release events evaluated using linescan imaging. Events presented here are limited to discrete, spatially symmetric Ca^{2+} release events (see Results). The mean values from permeabilized RyR3 ($n = 246$) versus RyR1 ($n = 151$) myotube cultures are as follows: amplitude (1.15 ± 0.04 vs. 0.97 ± 0.03; $\Delta F/F^{\ddagger}$), duration (17.48 ± 0.58 vs. 14.39 ± 0.36 ms FDHM‡), rise time (7.68 ± 0.29 vs. 7.73 ± 0.29 ms), and width (1.88 ± 0.05 vs. 1.80 ± 0.04 μm FWHM). ‡, $P < 0.05$

seem to be considerably more spatially restricted than those we observed in the same fibers before permeabilization. Previous simulations have shown that the spatial extent of increased fluorescence in a *xy* image of a Ca^{2+} spark depends on the rapidity of rise and fall of local fluorescence relative to the speed of acquisition of the *xy* image. Radially symmetrical fluorescence changes that rise and fall with a time course comparable with the rate of acquisition of successive lines in the *xy* image seem to be relatively compressed along the axis of slower scanning (Ward et al., 2000). Thus, the smaller mean area of increased fluorescence in the events after permeabilization could have been partially attributable to a faster rise and fall of fluorescence in these events. To address this possibility, linescan imaging was used to evaluate more precisely the temporal properties of the Ca^{2+} release events.

Figs. 9, *A* and *B* are representative linescan images from active areas of an intact (*A*) and subsequently permeabilized (*B*) RyR3-transduced myotube. Linescan imaging of intact myotubes revealed numerous foci of locally elevated fluorescence, which occurred as either spatially discrete elevations of fluorescence (*A*, *green arrowhead*) or as spatially more diffuse increases in fluorescence (*A*, *red arrowhead*). This included elevations of fluorescence that seem to originate from a discrete site and then propagate away for a short distance from the site of origin (*C*, large event in another myotube). Linescan imaging of the same myotube as in *A*, but after permeabilization and equilibration with fluo-3 (*B*), revealed almost exclusively discrete local increases in fluorescence and an absence of spatially propagated fluorescence increases. Thus, as in the case of the *xy* images before and after permeabilization, linescan *xt* imaging also revealed that the extent of spatial spread of spontaneous fluorescence increases in RyR3-transduced myotubes was more restricted after than before permeabilization. Quantitative spatiotemporal analysis of the events seen in the linescan images of the same RyR3-transduced myotubes before and after permeabilization was limited to spatially symmetric elevations in fluorescence (Fig. 9 *A*, *lower arrow*; *B*, all events). Asymmetric propagating increases in fluorescence (*top arrow* in *A*; spatially large event in *C*) were excluded because of our inability to adequately characterize these events based on our predefined independent measures (see Methods). Fig. 10 displays the population histograms of the four independent measures characterizing the discrete spatially symmetric elevations in

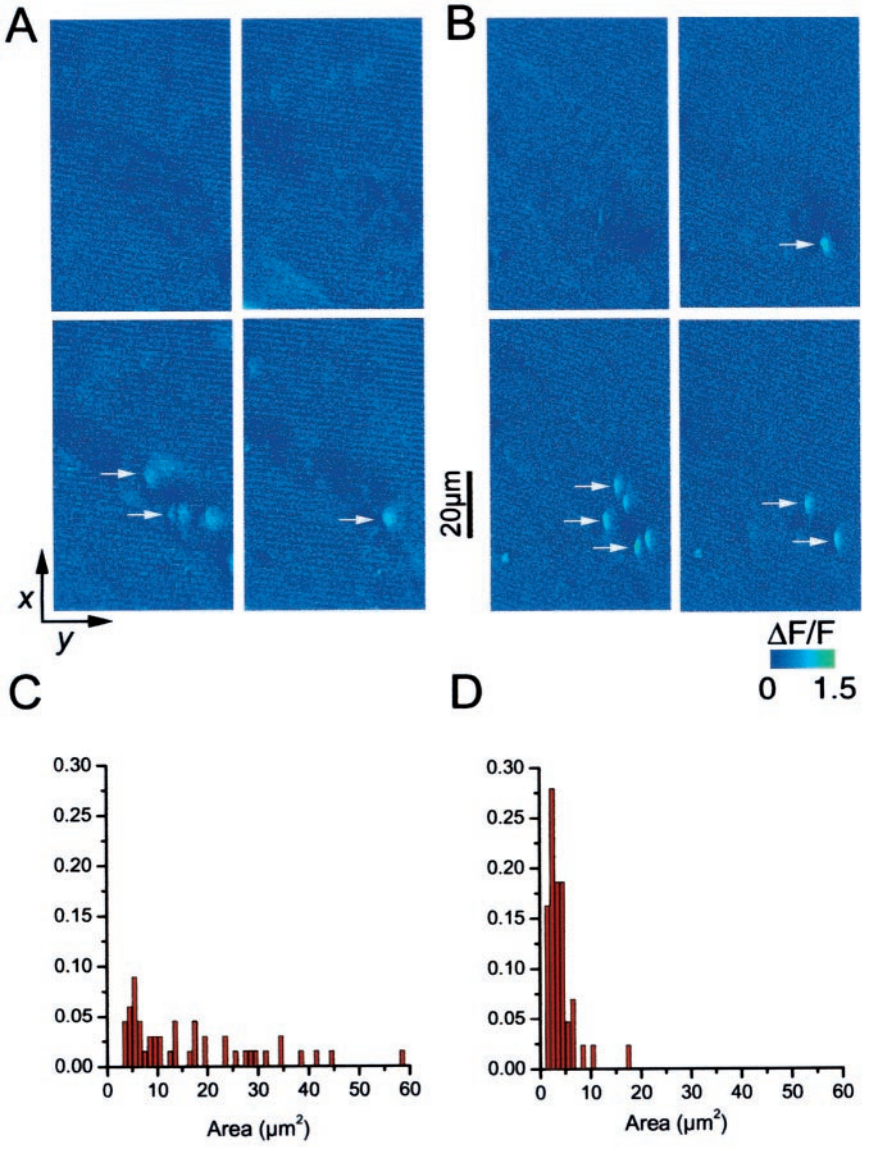

FIGURE 8 Spatial properties of Ca^{2+} release events from eight fluo-4–loaded RyR3-expressing 1B5 myotubes were evaluated in the intact preparation (*A*) and after subsequent permeabilization with saponin (*B*). (*A*) A sequence of 20 *xy* fluo-4 fluorescence images was collected from a random field of intact myotubes from a RyR3-infected culture. Four representative successive images in the sequence are shown as $\Delta F/F$ (*pseudocolor panels*). Arrows indicate identified events in both (*A*) and (*B*). (*B*) After permeabilization and equilibration with 50 μm fluo-3, 20 successive images were collected of the same field. The same portion of the active cell in (*A*) is visible in (*B*). After permeabilization, the proportion of discrete localized events is increased, with the appearance of reproducibly sized local events and a clear absence of the spatially extensive events seen in the intact cells (*A*). (*C* and *D*) Histograms present the distribution of event areas (the total area of all pixels in the identified event having values >0.5 of max $\Delta F/F$ in that event) in *xy* images of random fields from both intact (*C*) and permeabilized (*D*) RyR3-infected cells. Each condition is normalized to the total number of events (intact, $n = 89$; permeabilized, $n = 64$). The mean spatial area of all pixels having values at least 50% of the maximum $\Delta F/F$ in an event was 16.64 $\pm$ 2.64 μm^2 for intact myotubes and 4.02 $\pm$ 0.45 μm^2 ($P < 0.05$) after permeabilization.

fluorescence in linescan images from intact and permeabilized myotubes expressing RyR3. The mean values for rise time (4.12 $\pm$ 0.15 vs. 5.76 $\pm$ 0.29 ms), FDHM (23.29 $\pm$ 1.07 vs.31.51 $\pm$ 1.66 ms), and FWHM (3.66 $\pm$ 0.11 vs. 4.38 $\pm$ 0.16 μm) were all significantly smaller ($P < 0.05$) in permeabilized (*black bars*) versus intact (*open bars*) myotubes, respectively. In contrast, the mean amplitude of the events remained essentially the same in intact (0.81 $\pm$ 0.03 $\Delta F/F$) and permeabilized (0.83 $\pm$ 0.02 $\Delta F/F$) conditions. It is likely that either differing resting [Ca^{2+}] or altered Ca^{2+} buffering capacity of the fabricated internal solution compared with the cellular milieu contributed to much of the differences seen between the intact and permeabilized cells. However, it is unlikely that any differences in the Ca^{2+} indicators fluo-3 and fluo-4 were responsible for the differences in the event properties observed in intact

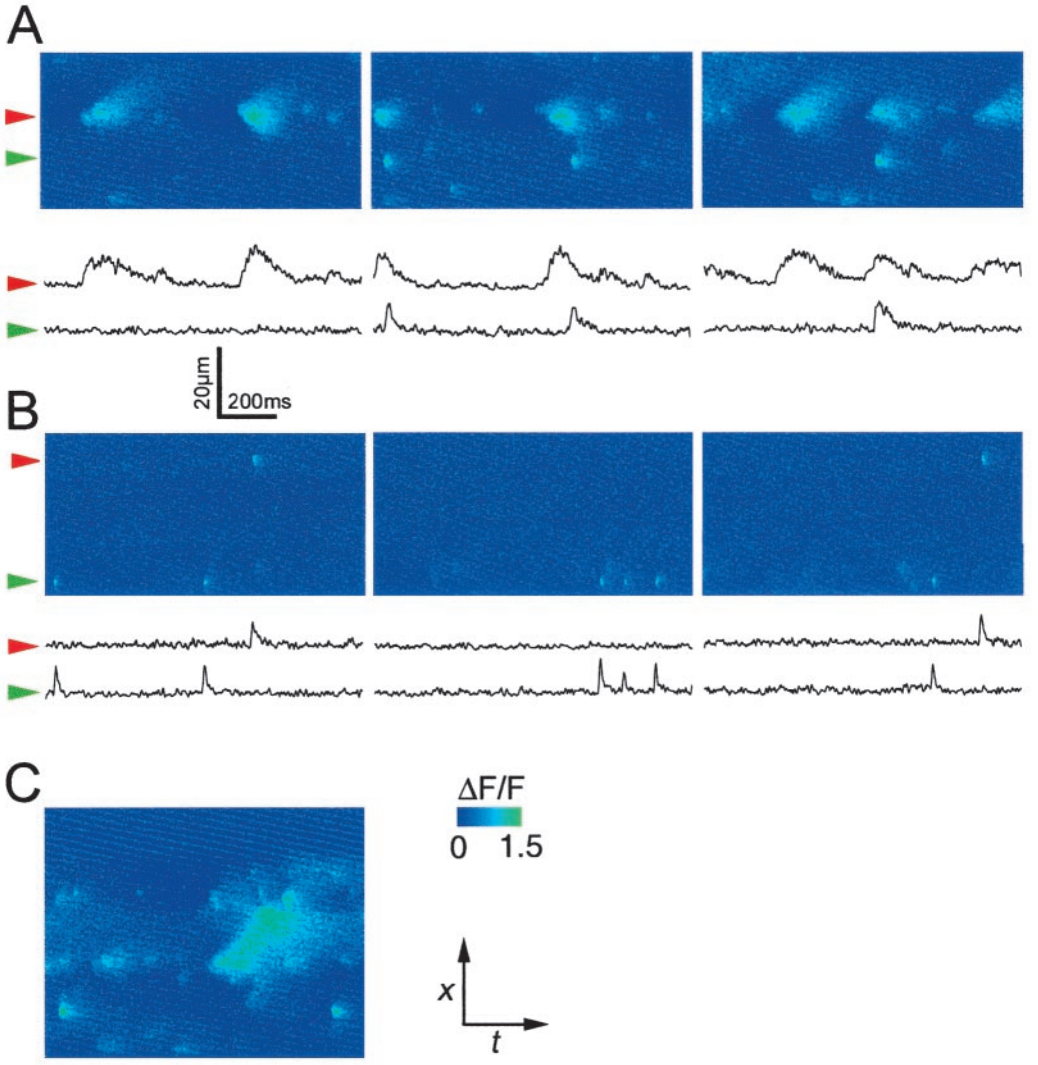

FIGURE 9 Representative linescan images from an intact (*A*) and subsequently permeabilized (*B*) RyR3-transduced myotube described in Fig. 2. Linescan imaging of intact myotubes (*A*) revealed numerous foci of Ca^{2+} release which occurred as either discrete Ca^{2+} release events (*A, green arrowhead*) or as spatially diffuse, propagating events (*A, red arrowhead*; *C,* large event). Linescan imaging of the same myotube (*A*), but after permeabilization and equilibration with fluo-3, revealed almost exclusively discrete Ca^{2+} release events of a stereotypic nature and an absence of spatially propagated Ca^{2+} release events.

myotubes containing fluo-4 and in permeabilized myotubes containing fluo-3. In our previous experience with permeabilized frog skeletal muscle preparations, these two indicators yield Ca^{2+} release events with similar spatiotemporal properties (unpublished observations).

Lack of Ca^{2+} release in cultures transduced with a Ca^{2+} insensitive RyR3 mutant ($RyR3_m$; E3885A)

1B5 myotube cultures transduced with $RyR3_m$ cDNA were probed for spontaneous Ca^{2+} release events. Successive *xy* scans of random fields within each intact (three cultures; 24 random fields) and permeabilized culture (three cultures; 28 random fields) revealed no discrete Ca^{2+} release events or whole-cell waves. These intact cells also did not release Ca^{2+} in response to 40 mM K^+ depolarization and neither group responded to 15 mM caffeine. These results are consistent with whole-cell responses seen when this protein was expressed in nonmuscle cells (Chen et al., 1999).

DISCUSSION

In this investigation we present the first direct comparison of the spontaneous Ca^{2+} release behavior of the recombinant skeletal muscle RyR isoforms, RyR1 and RyR3, in the same homologous expression system. We now demonstrate that myotubes transduced with RyR1 cDNA exhibit spontaneous elevations of cytosolic [Ca^{2+}] similar to those seen

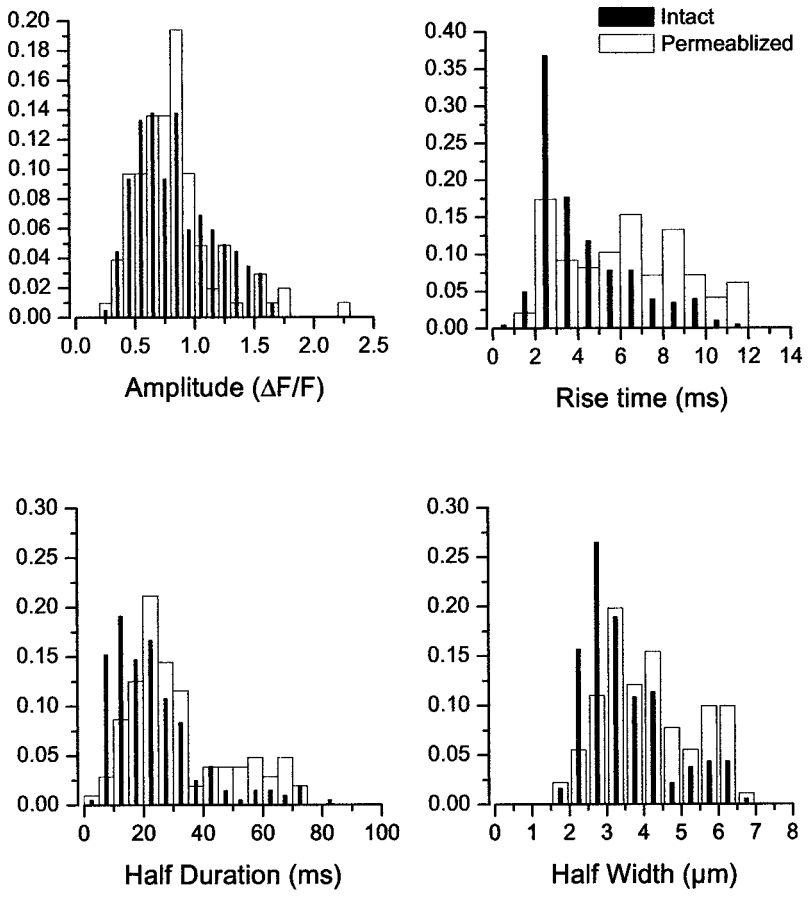

FIGURE 10 Histograms of spatiotemporal properties from discrete, spatially symmetric Ca^{2+} release events seen in the linescan images of intact and permeabilized RyR3-expressing myotube cultures. Asymmetric propagating release events (*top arrow* in Fig. 9 *A*; large event in Fig. 9 *C*) were excluded because of our inability to adequately characterize these events based on our predefined independent measures (see Methods). The mean values for rise time (5.76 ± 0.29, 4.12 ± 0.15 ms), FDHM (31.51 ± 1.66, 23.29 ± 1.07 ms), and FWHM (4.38 ± 0.16, 3.66 ± 0.11 μm) were all significantly smaller ($P < 0.05$) in intact (*black bars*) versus permeabilized (*open bars*), respectively. In contrast, the mean amplitude of the events remained unchanged between the intact (0.81 ± 0.03 $\Delta F/F$) and permeabilized (0.83 ± 0.02 $\Delta F/F$) conditions.

with expression of recombinant RyR3; however, these RyR1-dependent events occur much less frequently when examined under the same conditions as RyR3.

In permeabilized, fluo-3–loaded myotubes, RyR3 expression restored caffeine-induced Ca^{2+} release and caused the appearance of spontaneous, spatially localized elevations of cytosolic Ca^{2+}. These results confirm our previous report that in permeabilized myotubes, RyR3 alone was sufficient to induce spontaneous Ca^{2+} release events that are generally similar to those seen in frog muscle (Ward et al., 2000). We demonstrate that intact myotubes expressing RyR3 also exhibit local Ca^{2+} elevations as those seen in permeabilized RyR3-expressing myotubes yet the population parameters of these events exhibit smaller spatial and temporal characteristics.

We hypothesize that the spontaneous Ca^{2+} release events observed in the RyR3-expressing myotubes were ligand-activated by CICR and were independent of the DHPR based on several factors. First, the frequency of occurrence of local events in the RyR3-expressing 1B5 myotubes demonstrates sensitivity to caffeine and Mg^{2+} (Ward et al., 2000), which are the hallmark tests of CICR (Meissner, 1994). In these myotubes, although expression of RyR3 does result in the presence of surface couplings, it does not restore the appearance of organized DHPR tetrads (Protasi et al., 1999) and fails to restore depolarization-induced, DHPR-dependent Ca^{2+} release (Fessenden et al., 2000). Thus, it is unlikely that the RyR3 expressed in these dyspedic myotubes specifically interacts with the DHPRs, and the occurrence of local Ca^{2+} release events when RyR3 is expressed should be independent of the state of the voltage sensors.

1B5 myotube cultures transduced with RyR1 also exhibited spontaneous Ca^{2+} release events in both permeabilized and intact preparations. Our present findings represent the first report of recombinant RyR1 protein producing local-

ized Ca^{2+} release events in an expression system. A previous investigation (Bhat et al., 1997) has demonstrated that the transfection of full-length RyR1 cDNA into Chinese hamster ovary cells resulted in the appearance of a graded, global, caffeine-induced Ca^{2+} release response with an absence of discrete Ca^{2+} release events. Other investigations, however, have reported discrete Ca^{2+} release events in embryonic muscle fibers and primary myotube cultures that lack RyR3 and express only RyR1 (Conklin et al., 1999; Shirokova et al., 1999a, b). Taken together with our present results, these reports suggest that within a skeletal muscle context, RyR1 is capable of producing spontaneous Ca^{2+} release events in the absence of RyR3.

An evaluation of the properties of the Ca^{2+} release events between RyR3 and RyR1 was performed. Analysis of the spatial dimensions of the Ca^{2+} release area in *xy* scans revealed a larger spatial dimension of the Ca^{2+} release area in RyR1-expressing cells, with no difference in amplitude, suggestive of an increase in the spatial size of the Ca^{2+} release unit (i.e., number of RyRs) underlying the event. The variability in the spatial extent of the local areas of increased fluorescence in *xy* within each isoform may be partially attributable to the timing of the *xy* scan relative to the time of occurrence of the Ca^{2+} release event underlying the elevated local $[Ca^{2+}]$ (Ward et al., 2000).

Examination of the spontaneous Ca^{2+} release events with higher time-resolution line imaging was performed. Linescan imaging revealed both spatially symmetric, discrete spark-like events, and events which were nonstereotypic (i.e., long in duration, nonsymmetric, propagating, etc.). These types of events have been reported in both myotube preparations (Shirokova et al., 1999b; Ward et al., 2000) and permeabilized adult skeletal muscle preparations (unpublished observations).

Populations of events in RyR1 and RyR3, which were spatially symmetric and having a defined rising and decay phase (i.e., spark-like), were evaluated with our predefined criteria which have been previously used to evaluate local Ca^{2+} release events. (Klein et al., 1996; Ward et al., 2000; Shtifman et al., 2000). This analysis revealed that the population of events in RyR3-expressing myotubes was larger in amplitude and duration than the population seen in RyR1. This is in contrast to data by Conklin et al. (2000), who demonstrated that Ca^{2+} sparks from RyR1 or RyR3 KO embryonic muscle were similar in spatiotemporal properties. It is important to note that in our current study, certain experimental limitations were realized in collecting and evaluating the linescan data. First, linescan imaging was performed on myotubes that were previously identified as having spontaneous activity; therefore, the scan-line placement was not randomized. Secondly, numerous nonstereotypic events were collected in both RyR1- and RyR3-expressing myotubes that could not be analyzed with our predetermined criteria. In fact, the variability of the types of events collected precluded us from categorizing these events into distinct populations. Despite these limitations, we can conclude that both RyR1 and RyR3 proteins are capable of producing localized spontaneous Ca^{2+} release events and that a subpopulation of these events resemble the Ca^{2+} spark type release previously reported in other striated muscle systems (see Introduction).

The frequency of occurrence of events was much lower in random fields of intact or permeabilized dyspedic myotubes expressing RyR1 than in random fields of dyspedic myotubes expressing RyR3 (see Results), although the pattern and level of RyR expression was similar for both isoforms. The relatively low occurrence rate and regional localization of Ca^{2+} release behavior seen here has also been previously reported in embryonic skeletal muscle fibers (Conklin et al., 1999; Chun et al., 2001) and in cultured myotubes (Shirokova et al., 1999b; Ward et al., 2000), which also display isolated regions exhibiting spontaneous Ca^{2+} release events. Exposure of RyR1-expressing myotubes to low levels of caffeine resulted in no detectable change in the frequency of spontaneous local Ca^{2+} release events. This is in contrast to the ability of the same levels of caffeine to increase the frequency of Ca^{2+} release events in RyR3-expressing cells (Ward et al., 2000). However, it is consistent with the lower sensitivity of RyR1 for CICR compared with RyR3 as has been previously reported (Chen et al., 1999; Murayama et al.,1999; Fessenden et al., 2000; Conklin et al., 2000).

In addition to the spontaneous elevations of local $[Ca^{2+}]$ observed in RyR1-expressing dyspedic myotubes in these studies, the RyR1-expressing myotubes also exhibited another form of Ca^{2+} release. This was indicated by the observation that in the RyR1-expressing myotubes, lowered cytosolic $[Mg^{2+}]$ increased the ambient global $[Ca^{2+}]$ in the absence of detectable local events. This observation indicates that in RyR1-expressing myotubes, there may have been numerous local Ca^{2+} release events that were too small to produce detectable local elevations of $[Ca^{2+}]$. Previous reports have also identified similar forms of Ca^{2+} release (i.e., lack of discrete events) in voltage-clamped adult rat skeletal muscle and myotubes that contained RyR1 solely (Shirokova et al., 1998, 1999b). In contrast, both 0.25 mM caffeine and lowered $[Mg^{2+}]$ did increase the frequency of detected events in RyR3-expressing myotubes without an increase in global $[Ca^{2+}]$ (Ward et al., 2000). Thus, it seems that the basic increments of Ca^{2+} release in RyR3-expressing myotubes produce detectable local $[Ca^{2+}]$ elevations, whereas the basic increments of Ca^{2+} release in RyR1-expressing myotubes do not. A possible basis for this difference may be related to the ease of propagation of activation between neighboring RyRs in a cluster, assuming RyRs coupled to DHPRs to be less likely to be activated by CICR than uncoupled RyRs. In the RyR1 clusters that generated the postulated undetectable increments of Ca^{2+} release underling the observed global increase in $[Ca^{2+}]$ in RyR1 expressing myotubes, alternate RyRs are either cou-

pled to DHPRs, and thus possibly unavailable for activation during spontaneous release, or uncoupled and available for release. In contrast, in the RyR clusters in RyR3-expressing myotubes, all RyRs are uncoupled to DHPRs (Protasi et al., 2000) and, thus, possibly available for release activation. Thus, RyR3 clusters could generate detectable basic increments of Ca^{2+} release attributable to more extensive propagation of activation between neighboring RyR3s in a cluster, whereas RyR1-expressing myotubes with a majority of alternate RyRs coupled to DHPRs might generate much smaller increments of Ca^{2+} release (i.e., undetectable as a discrete release event) because of less effective spread of activation within the cluster.

Neither partial depolarization of intact RyR1-expressing myotubes with 7 mM K^+ nor application of nifedipine, which promotes inactivation of the TT voltage sensors (Rios and Brum, 1987), caused changes in event frequency in RyR1-expressing myotubes. Based on this finding, we hypothesize that the spontaneous Ca^{2+} release events detected in RyR1-expressing myotubes were independent of the DHPRs. This hypothesis is supported by a report by Shirokova et al. (1999b) which demonstrates that the discrete Ca^{2+} release events they saw in RyR3 KO myotubes were produced by "islands" of RyR1 channels, which they hypothesized were uncoupled to DHPR voltage sensors.

Application of 40 mM K^+ to intact RyR1-expressing myotubes, however, did elicit a global Ca^{2+} release, indicating that RyR1 expression in these cells did restore skeletal DHPR-RyR E-C coupling mechanisms as previously described in this 1B5 system (Protasi et al., 1998). Because expression of RyR1 restores skeletal type E-C coupling and the tetradic arrangement of DHPRs (Protasi et al., 1998, 1999), we conclude that the low frequency of spontaneous local elevations of $[Ca^{2+}]$ in intact and permeabilized RyR1-expressing myotubes is most probably attributable to an inhibitory influence of the DHPRs on RyR1. Alternatively, the relatively low frequency of events in RyR1 compared with RyR3-expressing myotubes might reflect a fundamental difference in the Ca^{2+} release behavior between the two isoforms.

SUMMARY

Our results indicate that in the dyspedic myotube system, which lacks RyRs but retains accessory E-C coupling proteins, expression of recombinant RyR1 or RyR3 produces spontaneous local elevations of cytosolic $[Ca^{2+}]$. Furthermore, differences in the spatiotemporal properties and the frequency of occurrence of localized Ca^{2+} release events underscore functional differences between the Ca^{2+} release behavior of RyR1 and RyR3 in this homologous expression system.

REFERENCES

Airey, J. A., C. F. Beck, K. Murakami, S. J. Tanksley, T. J. Deerinck, M. H. Ellisman, and J. L. Sutko. 1990. Identification and localization of two triad junctional foot protein isoforms in mature avian fast twitch skeletal muscle. *J. Biol. Chem.* 265:14187–14194.

Bertocchini, F., C. E. Ovitt, A. Conti, V. Barone, H. R. Scholer, R. Bottinelli, C. Reggiani, and V. Sorrentino. 1997. Requirement for the ryanodine receptor type 3 for efficient contraction in neonatal skeletal muscles. *EMBO J.* 16:6956–6963.

Bhat, M. B., J. Zhao, W. Zang, W. Balke, H. Takeshima, W. G. Wier, and J. Ma. 1997. Caffeine-induced release of intracellular Ca^{2+} from Chinese hamster ovary cells expressing skeletal muscle ryanodine receptor. *J. Gen. Phys.* 110:749–762.

Block, B. A., T. Imagawa, K. P. Campbell, and C. Franzini-Armstrong. 1988. Structural evidence for direct interaction between the molecular components of the transverse tubule/sarcoplasmic reticulum junction in skeletal muscle. *J. Cell Biol.* 107:2587–2600.

Brum, G., A. Gonzalez, J. Rengifo, N. Shirokova, and E. Rios. 2000. Fast imaging in two dimensions resolves extensive sources of Ca^{2+} sparks in frog skeletal muscle. *J. Physiol.* 528:419–433.

Cannell, M. B., and C. Soeller. 1999. Mechanisms underlying Ca^{2+} sparks in cardiac muscle. *J. Gen. Phys.* 113:373–379.

Chandler, W. K., R. F. Rakowski, and M. F. Schneider. 1976. Effects of glycerol treatment and maintained depolarization on charge movement in skeletal muscle. *J. Physiol.* 254:285–316.

Chen, S. R., K. Ebisawa, X. Li, L., and Zhang. 1999. Molecular identification of the ryanodine receptor Ca^{2+} sensor. *J. Biol. Chem.* 273: 14675–14678.

Cheng, H., W. J. Lederer, and M. B. Cannell. 1993. Ca^{2+} sparks: elementary events underlying excitation contraction coupling in heart muscle. *Science.* 262:740–744.

Cheng, H., L. Song, N. Shirokova, A. Gonzalez, E. G. Lakatta, E. Rios, and M. D. Stern. 1999. Amplitude distribution of calcium sparks in confocal images: theory and studies with an automatic detection method. *Biophys. J.* 76:606–617.

Chun, L., C. W. Ward, and M. F. Schneider. 2001. Ca^{2+} influx and local Ca^{2+} events in mammalian embryonic skeletal muscle. *Biophys. J.* 80:65A.

Csernoch, L., V. Jacquemond, and M. F. Schneider. 1993. Microinjection of strong calcium buffers suppresses the peak of calcium release during depolarization in frog skeletal muscle fibers. *J. Gen. Physiol.* 101: 297–333.

Conklin, M. W., P. Powers, R. G. Gregg, and R. Coronado. 1999a. Ca^{2+} sparks in embryonic skeletal muscle myotubes selectively deficient in dihydropyridine receptor $\forall_{1S}$ or $\exists_{1a}$ subunits. *Biophys. J.*76:657–669.

Conklin, M., V. Barone, V. Sorrentino, and R. Coronado. 1999b. Contribution of ryanodine receptor type 3 to Ca^{2+} sparks in embryonic skeletal muscle. *Biophys. J.* 77:1394–1403.

Conklin, M. W., C. A. Ahern, P. Vallejo, V. Sorrentino, H. Takeshima, and R. Coronado. 2000. Comparison of Ca^{2+} sparks produced independently by two ryanodine receptor isoforms (type 1 or type 3). *Biophys. J.* 78:1777–1785.

Conti, A., L. Gorza, and V. Sorrentino. 1996. Differential distribution of ryanodine receptor type 3 (RyR3) gene product in mammalian skeletal muscles. *Biochem. J.* 316:19–23.

Fessenden, J., Y. Wang, R. A. Moore, S. R. W. Chen, P. D. Allen, and I. N. Pessah. 2000. Divergent physiological and pharmacological properties of ryanodine receptor types 1 and 3 expressed in a myogenic cell line. *Biophys. J.* 79:2509–2525.

Flucher, B. E., A. Conti, H. Takeshima, and V. Sorrentino. 1999. Type 3 and type 1 ryanodine receptors are localized in triads of the same mammalian skeletal muscle fibers. *J. Cell Biol*. 146:621–630.

Fraefel, C., S. Song, F. Lim, P. Lang, L. Yu, Y. Wang, P. Wild, and A. I. Geller. 1996. Helper virus-free transfer of herpes simplex virus type 1 plasmid vectors into neural cells. *J. Virol.* 70:7190–7197.

Klein, M. G., H. Cheng, L. F. Santana, Y. H. Jiang, W. J. Lederer, and M. F. Schneider. 1996. Two mechanisms of quantized calcium release in skeletal muscle. *Nature.* 379:455–458.

Lorenzon, P., F. Grohovaz, and F. Ruzzier. 2000. Voltage- and ligand-gated ryanodine receptors are functionally separated in developing C2C12 mouse myotubes. *J. Physiol.* 525:499–507

Meissner, G. 1994. Ryanodine receptor/Ca^{2+} release channels and their regulation by endogenous effectors. *Annu. Rev. Physiol.* 56:485–508.

Moore, R. A., J. D. Fessenden, Y. Wang, S. R. Chen, P. D. Allen, and I. N. Pessah. 1999. Viral expression of RYR1 and RYR3 in a myogenic cell line lacking native RyR. *Biophys. J.* 76:A394.

Moore, R. A., H. Nguyen, J. Galceran, I. N. Pessah, and P. D. Allen. 1998. A transgenic myogenic cell line lacking ryanodine receptor protein for homologous expression studies: reconstitution of Ry1R protein and function. *J. Cell Biol.* 140:843–851.

Murayama, T., T. Oba, E. Katayama, H. Oyamada, K. Oguchi, M. Kobayashi, K. Otsuka, and Y. Ogawa. 1999. Further characterization of the type 3 ryanodine receptor (RyR3) purified from rabbit diaphragm. *J. Biol. Chem.* 274:17297–17308.

Nakai, J., R. T. Dirksen, H. T. Nguyen, I. N. Pessah, K. G. Beam, and P. D. Allen. 1996. Enhanced dihydropyradine receptor channel activity in the presence of ryanodine receptor. *Nature.* 380:72–75.

Protasi, F., C. Franzini-Armstrong, and P. D. Allen. 1998. Role of ryanodine receptors in the assembly of calcium release units in skeletal muscle. *J. Cell Biol.* 140:831–842.

Protasi, F., C. Franzini-Armstrong, and B. E. Flucher. 1997. Coordinated incorporation of skeletal muscle dihydropyridine receptors and ryanodine receptors in peripheral couplings of BC3H1 cells. *J. Cell Biol.* 137:859–870.

Protasi, F., H. Takekura, S. R. Chen, C. Franzini-Armstrong, and P. D. Allen. 1999. RyR3 expression in a dyspedic cell line does not restore junctional DHPR-tetrads. *Biophys. J.* 76:A470.

Protasi, F., H. Takekura, Y. Wang, S. R. Chen, G. Meissner, P. D. Allen, and C. Franzini-Armstrong. 2000. RyR1 and RyR3 have different roles in the assembly of calcium release units of skeletal muscle. *Biophys. J.* 79:2494–2508.

Rios, E., and G. Brum. 1987. Involvement of dihydropyridine receptors in excitation-contraction coupling in skeletal muscle. *Nature*. 325: 717–720.

Rios, E., and G. Pizarro. 1988. Voltage sensors and calcium channels of excitation-contraction coupling. *NIPS* 223–228.

Schneider, M. F. 1999. Ca^{2+} sparks in frog skeletal muscle: generation by one, some, or many SR Ca^{2+} release channels? *J. Gen. Physiol.* 113: 365–372.

Schneider, M. F., and W. K. Chandler. 1973. Voltage dependent charge movement in skeletal muscle. *Nature.* 242:244–246.

Shirokova, N., J. Garcia, and E. Rios. 1998. Local calcium release in mammalian skeletal muscle *J. Physiol.* 512:377–384.

Shirokova, N., A. Gonzalez, W. G. Kirsch, E. Rios, G. Pizarro, M. D. Stern, H. Cheng. 1999a. Calcium sparks: release packets of uncertain origin and fundamental role. *J. Gen. Physiol.* 113:377–384.

Shirokova, N., R. Shirokov, D. Rossi, A. Gonzalez, W. G. Kirsch, J. Garcia, V. Sorrentino, and E. Rios. 1999b. Spatially segregated control of Ca^{2+} release in developing skeletal muscle of mice. *J. Physiol.* 521:483–495.

Shtifman, S., C. W. Ward, J. Wang, H. H. Valdivia, and M. F. Schneider. 2000. Effects of imperatoxin A on local sarcoplasmic reticulum Ca^{2+} release in frog skeletal muscle. *Biophys. J.* 79:814–827.

Sonnleitner, A., A. Conti, F. Bertocchini, H. Schindler, and V. Sorrentino. 1998. Functional properties of the ryanodine receptor type 3 (RyR3) Ca^{2+} release channel. *EMBO J.* 17:2790–2798.

Sutko, J. L., and J. A. Airey. 1996. Ryanodine receptor Ca^{2+} release channels: does diversity in form equal diversity in function? *Phys. Rev.* 76:1027–1071.

Tsugorka, A., E. Rios, and L. A. Blatter. 1995. Imaging elementary events of Ca^{2+} release in skeletal muscle cells. *Science.* 269:1723–1726.

Wang, Y., C. Fraefel, F. Protasi, R. A. Moore, J. D. Fessenden, I. N. Pessah, A. DiFrancesco, X. Breakefield, and P. D. Allen. 2000. HSV-1 amplicon vectors are a highly efficient gene delivery system for skeletal muscle myoblasts and myotubes. *Am. J. Physiol. Cell Physiol.* 278: C619—C626.

Ward, C. W., A. Lacampagne, M. G. Klein, and M. F. Schneider. 1998. Ca^{2+} spark properties in saponin permeabilized skeletal muscle fibers. *Biophys. J.* A269.

Ward, C. W., M. F. Schneider, D. Castillo, F. Protasi, Y. Wang, and P. D. Allen. 2000. Expression of ryanodine receptor RyR3 produces Ca^{2+} sparks in dyspedic myotubes *J. Physiol.* 525:91–103.